VECTOR FIELD CONVOLUTION FOR IMAGE SEGMENTATION USING SNAKES

Bing Li and Scott T. Acton

{bingli, acton}@virginia.edu
University of Virginia, Charlottesville, VA 22904 USA

ABSTRACT

Snakes, or *active contours*, have been widely used in image processing applications. Typical roadblocks to consistent performance include limited capture range, noise sensitivity, and poor convergence to concavities. This paper proposes a new design for the snake external force, called vector field convolution (VFC), to address these problems. Qualitative and quantitative comparisons with the gradient vector flow (GVF) external force are presented in this paper to show the advantages of this innovation.

Index Terms — Image processing, image segmentation, image shape analysis, object detection

1. INTRODUCTION

Snakes [1] (a.k.a. *active contours*) have been widely used for image segmentation [2] and tracking [3, 4]. Snakes can deform on the image domain and capture a desired object boundary. The snake evolution is achieved via minimizing an energy functional subject to physically meaningful constraints. The energy functional usually contains two terms: an internal energy, which constrains the smoothness and tautness of the surface, and an external energy, which attracts the surface to the features of interest.

An external force design for snakes called *gradient vector flow* (GVF) [5] and its improved version in [6] were introduced to accommodate a large capture range and to enable faithful representation of curve concavities. Although GVF has been widely used, there are some disadvantages, such as noise sensitivity, parameter sensitivity, high computational cost and the esoteric relationship between the capture range and parameters.

In this paper, we present a novel external force implementation for snakes called *vector field convolution* (VFC). This external force field is calculated by convolving a vector field kernel with the edge map derived from the gray-level or binary image. Snakes that use the VFC external force are termed VFC snakes. Similar to the GVF approach, instead of being formulated using the standard energy minimization framework, VFC snakes are constructed by way of a force balance condition.

Advantages of VFC snakes over GVF snakes are insensitivity to noise and initialization, flexibility of changing the capture range in a meaningful way, and reduced computational cost. Those advantages are demonstrated by examples and comparisons with GVF snakes in Section 4.

2. BACKGROUND

An active contour is represented by a parametric curve $\mathbf{x}(s)=\left[x(s),y(s)\right]$, $s\in[0,1]$, that deforms through the image domain to minimize the energy functional

$$E_{\text{AC}}=\int_0^1\left[\frac{1}{2}\left(\alpha\left|\mathbf{x}'(s)\right|^2+\beta\left|\mathbf{x}''(s)\right|^2\right)+E_{\text{ext}}\left(\mathbf{x}(s)\right)\right]ds \quad (1)$$

where α and β are weight parameters representing the smoothness and tautness degrees of the contour, respectively, and $\mathbf{x}'(s)$ and $\mathbf{x}''(s)$ are the first and second derivatives of $\mathbf{x}(s)$ with respect to s. E_{ext} denotes the external energy, the value of which is small at the features of interest [5]. To minimize (1), the contour must satisfy the Euler equation

$$\alpha\mathbf{x}''(s)-\beta\mathbf{x}''''(s)-\nabla E_{\text{ext}}=0 \quad (2)$$

where ∇ is the gradient operator. This can be considered as a force balance equation

$$\mathbf{F}_{\text{int}}+\mathbf{F}_{\text{ext}}=0 \quad (3)$$

where $\mathbf{F}_{\text{int}}=\alpha\mathbf{x}''(s)-\beta\mathbf{x}''''(s)$ is the internal force to constraint the contour smoothness and $\mathbf{F}_{ext}=-\nabla E_{\text{ext}}$ is the external force to attract the contour toward the features of interest.

The *gradient vector flow* (GVF) field is the vector field $\overline{\mathbf{v}}(x,y)=\left[\overline{u}(x,y),\overline{v}(x,y)\right]$ that minimizes the energy functional

$$E_{\text{GVF}}=\iint\left[\mu\left(\left|\nabla\overline{u}\right|^2+\left|\nabla\overline{v}\right|^2\right)+\left|\nabla f\right|^2\left|\overline{\mathbf{v}}-\nabla f\right|^2\right]dxdy \quad (4)$$

where $f=-E_{\text{ext}}$ is an *edge map* derived from the image, and μ is a weight parameter controlling the degree of smoothness of the GVF field. As shown in [5], the GVF field has a large capture range and the ability to progress into concavities. Although the GVF field has several desired properties, there are still several unsolved problems, such as

the sensitivity to the parameters, the obscure relationship between the capture range and the parameters, the capture range sensitivity to noise, especially impulse noise, and expensive computational cost.

In this paper, we present a new design for a static external force that does not depend on the position of the active contour or change over time. This new external force, called *vector field convolution* (VFC), is calculated by convolving a vector field kernel with the edge map derived from the image. This novel external force has not only a large capture range and ability to converge to concavities, but also better robustness to noise and initialization, flexibility of changing the force field, and reduced computational cost.

3. VECTOR FIELD CONVOLUTION

We define a *vector field kernel* $\mathbf{k}(x,y)=\left[s(x,y),t(x,y)\right]$ in which all the vectors point to the origin

$$\mathbf{k}(x,y)=m(x,y)\mathbf{n}(x,y) \tag{5}$$

where $m(x,y)$ is the magnitude of the vector at (x,y) and $\mathbf{n}(x,y)$ is the unit vector pointing to the origin

$$\mathbf{n}(x,y)=\left[-x/r,-y/r\right] \tag{6}$$

where $r=\sqrt{x^2+y^2}$ is the distance from the origin, except that $\mathbf{n}(0,0)=[0,0]$ at the origin. A desirable external force should have an important property: a free particle placed in the field should be able to move to the features of interest, such as edges. If the origin is considered as the feature of interest, this vector field possesses this desirable property.

The vector field convolution (VFC) external force $\mathbf{v}(x,y)=\left[u(x,y),v(x,y)\right]$ is given by calculating the convolution of the vector field kernel $\mathbf{k}(x,y)$ and the edge map $f(x,y)$ generated from the image $I(x,y)$

$$\begin{aligned}\mathbf{v}(x,y)&=f(x,y)*\mathbf{k}(x,y)\\&=\left[f(x,y)*s(x,y),f(x,y)*t(x,y)\right]\end{aligned} \tag{7}$$

where $*$ denotes convolution. Since edge map $f(x,y)$ is larger near the image edges, edges contribute more to the VFC than homogeneous regions. Therefore, the VFC external force can move free particles to the edges.

The VFC field is strongly dependent on the magnitude of the vector field kernel $m(x,y)$. By considering the fact that the influence from the feature of interest should be less as the particles are further away, the magnitude should be a decreasing function of distance from the origin. We propose two types of magnitude functions, given as

$$m_1(x,y)=(r+\varepsilon)^{-\gamma}, \tag{8}$$

$$m_2(x,y)=\exp\left(-r^2/\sigma^2\right) \tag{9}$$

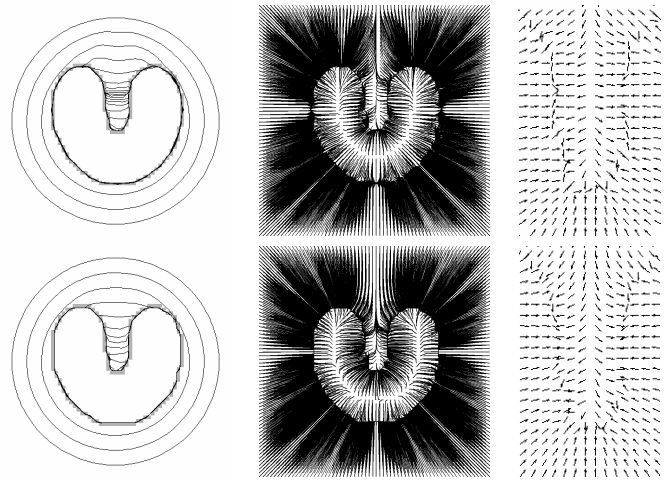

Fig. 1. Top (bottom) row, from left to right: convergence of GVF (VFC) snake, streamlines generated from GVF (VFC) field, and zoomed GVF (VFC) field within the concavity.

where γ and σ are positive parameters to control the decrease, ε is a small positive constant to prevent division by zero at the origin. $m_1(x,y)$ is inspired by Newton's law of universal gravitation in physics, which can be viewed as a special case with $\gamma=2$ and $\varepsilon=0$. The influence of features of interest decreases as γ increases. The magnitude function $m_2(x,y)$ is Gaussian-like, where σ can be viewed as the scale parameter. The influence of features of interest increases as σ increases. Note that the external force proposed in [7] is a special case of $m_1(x,y)$ with $\gamma=2$.

4. RESULTS AND ANALYSIS

Several examples in this section demonstrate desirable properties of the VFC snakes. The GVF snakes have gained tremendous popularity due to their ability to address a few difficulties appeared in previous instantiations of the active contour. Therefore, we also compare the VFC snake results with the GVF snake results. The magnitude function used in those experiments is $m_1(x,y)$ with $\gamma=2.4$.

4.1. Capture Range and Convergence to Concavity

We use the U-shape example, which is also shown in [5], in our experiment. As shown in Fig. 1, both the VFC snake and the GVF snake have a large capture range and concavity converge property. The two force fields are barely distinguishable from each other in this example; especially the vectors within the concavity in both force fields have a downward component to attract the snakes to the concavity.

In practical implementation, the capture range of the GVF field is determined by two parameters: the smoothness parameter μ and the number of iterations. Although we

know that the capture range increases as μ and the number of iterations increase, there is no specified relationship available to the user. In contrast, the capture range of the VFC field is determined by the maximum distance between any non-zero vector and the origin in the vector field kernel.

4.2. Initialization

As we see in Fig. 1, the snakes can be initialized far away outside the object for both the VFC snakes and the GVF snakes. Fig. 2 shows a set of initialization placed across and inside the boundary, with which both snakes converge.

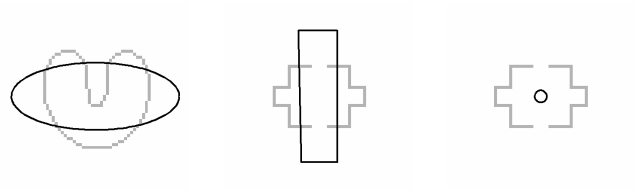

Fig. 2. Initializations with which both snakes converge.

4.3. Noise Sensitivity

To test the noise sensitivity of GVF snakes and VFC snakes, we add impulse noise to the U-shape image in Fig. 1. Fig. 3 illustrates the noisy image with initial snakes plotted in dash lines. The GVF snake in Fig. 3(a) fails to converge to the U-shape because it is distracted by local impulse noise. Although a better initialization provides an improved result in Fig. 3(b), the GVF snake does not capture some boundary features precisely, such as the concavity and bottom right portion, which are distorted by the Gaussian filter. However, the Gaussian filter is necessary to suppress the noise for the GVF snakes. The VFC snake converges to the desired features without using Gaussian filter, shown in Fig. 3(c). To quantify the accuracy of the results, the root mean square error (RMSE) of the snake is calculated. The error of a point in the snake is defined by the minimum distance between the point and U-shape in the noise-free image. These results reveal the superior robustness to noise afforded by VFC.

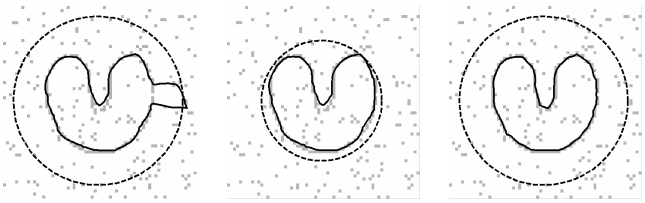

(a) RMSE = 3.20 (b) RMSE = 0.64 (c) RMSE = 0.53

Fig. 3. Impulse noise corrupted U-shape image with the initial snake (dash line) and the result (solid line); (a) and (b) the GVF snakes using edge map $f(x,y) = -G_5(x,y) * I(x,y)$, where $G_\sigma(x,y)$ is a 2D Gaussian function with standard deviation σ; (c) the VFC snakes using edge map $f(x,y) = -I(x,y)$.

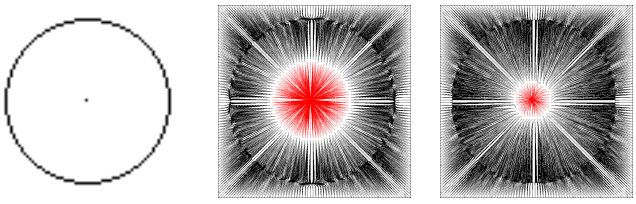

(a) (b) (c)

Fig. 4. (a) Circle with an impulse at the center; streamlines generated from (b) GVF field and (c) VFC field.

In other words, the capture range of GVF snakes is significantly affected by the noise, while the capture range of VFC snakes is not. The reason is that GVF only diffuses the gradient vectors without considering the "strength" of the features. On the other hand, strong or large features contribute more to the VFC field than weak and small features. We demonstrate this sensitivity in Fig. 4, where the input image consists of an impulse surrounded by a circle. From the streamlines generated from GVF and VFC, we can see white rings, which are the watersheds for capture ranges. The area outside the rings is the capture range for the circle, and the one inside is the capture range for the noise. As may be observed in the Fig. 4, noise has a diminished impact on the VFC field, compared to the response of the GVF field.

4.4. Flexibility

The magnitude function can be modified to provide a tailored VFC field. We can add an anisotropic term to obtain a VFC field similar to the motion gradient vector flow (MGVF) proposed in [3], which incorporates the motion direction inside the GVF energy to track cells. The modified VFC magnitude function is given as

$$m_3(x,y) = c(x,y)\, m_i(x,y), i = 1,2 \tag{10}$$

where $c(x,y)$ is the anisotropic term. In this experiment, $c(x,y)$ is given as

$$c(x,y) = 1/\left[2 - \mathbf{d} \bullet \mathbf{n}(x,y)\right] \tag{11}$$

where $\mathbf{d}$ is a unit vector representing the motion direction, $\bullet$ denotes the vector dot product. If $\mathbf{n}(x,y)$ and $\mathbf{d}$ have the same direction, $c(x,y)$ is close to 1; if they have opposite direction, $c(x,y)$ is close to 1/3. Therefore, the resulting VFC is biased in the motion direction.

Fig. 5(a) shows a synthetic cell image with a displaced initialization. The GVF snake fails to capture the proper boundary because of the isotropic force field, shown in Fig. 5(c). Fig. 5(b) shows that the VFC snake succeeds by using anisotropic magnitude function, where the motion direction is $\mathbf{d} = [-1, 0]$. The resulting anisotropic VFC force field is illustrated in Fig. 5(d). This example demonstrates that the VFC could be easily modified for different applications.

Table 1. CPU time and capture range for a 511^2 image.

GVF	Number of iterations	128	256	512
	CPU time (seconds)	4.47	8.88	22.6
	Capture range (pixels)	127	174	231
VFC	Kernel size (pixels)	127	255	511
	CPU time (seconds)	1.31	1.86	2.36
	Capture range (pixels)	90	181	362

4.5. Real Image Results

We apply the VFC snakes to noisy magnetic resonance (MR) images of human ankles. As shown in Fig. 6(a), the GVF snake is stuck in the interior and does not converge to edges. The reason can be found in Fig. 6(c) – the GVF snake tends to move in the vertical direction because there is no horizontal force component in the center area. Again, this is caused by the nature of GVF – gradient vector diffusion. In contrast, the VFC snake converges to the concavities on the bottom-right precisely, shown in Fig. 6(b). We also note that the GVF snake converges if the initialization is closer to the boundary. This anecdotal case exemplifies the robustness to initialization afforded by the VFC approach.

4.6. Computational cost

If we represent the vectors with complex numbers, the VFC field can be calculated by convolving a complex function with a real function. This convolution can be implemented via the fast Fourier transform (FFT), which can significantly reduce the computational expense when the kernel size is large. The computational cost of GVF mainly depends on the number of iterations, while the expense of VFC mainly depends on the size of the vector field kernel. Table 1 compares the computational cost and capture range of VFC with GVF. A 511 x 511 image, which has an intensity of one at the center and is zero–valued elsewhere, is used as the edge map. The capture range is defined as the maximum distance between a non-zero vector in the force field and the center. From Table 1, we may observe that GVF requires 3 to 10 times more computational expense than VFC with a similar capture range. This experiment was based on a Dell Precision 330 work station with P4 1.6GHz CPU, 1GB RAM and MATLAB code.

5. CONCLUSION

A novel external force for active contours, called the vector field convolution (VFC), has been introduced. The field is calculated by convolving a vector field with the edge map generated from the image. We have shown that the VFC snakes converge to boundary concavities, and have large capture ranges, similar to the GVF snakes. Furthermore, the VFC snakes are more robust to noise and initialization, more flexible, and less expensive than GVF snakes.

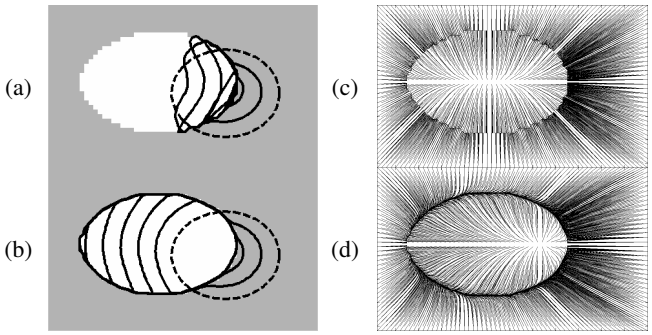

Fig. 5. An ellipse representing a synthetic cell with initial snakes (dash lines) and results (solid lines) using (a) GVF and (b) VFC; streamlines generated from (c) GVF field and (d) VFC field.

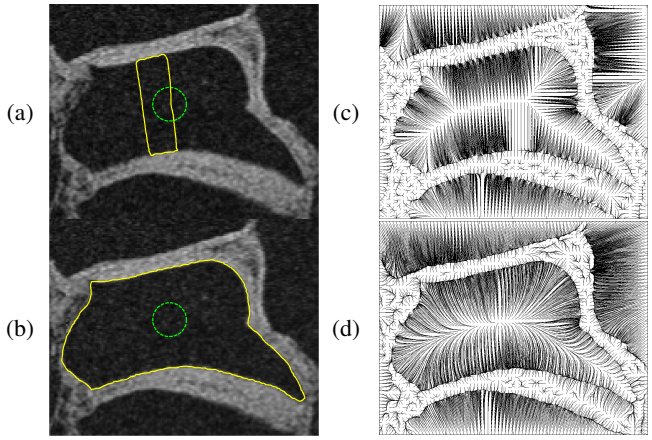

Fig. 6. MR image of a human ankle with initial snakes (dash lines) and results (solid lines) using (a) GVF and (b) VFC; streamlines generated from (c) GVF field and (d) VFC field.

REFERENCES

[1] M. Kass, A. Witkin, and D. Terzopoulos, "Snakes - active contour models," *International Journal of Computer Vision*, vol. 1, pp. 321-331, 1987.

[2] G. Dong, N. Ray, and S. T. Acton, "Intravital leukocyte detection using the gradient inverse coefficient of variation," *IEEE Trans. Medical Imaging*, vol. 24, pp. 910-924, 2005.

[3] N. Ray and S. T. Acton, "Motion gradient vector flow: an external force for tracking rolling leukocytes with shape and size constrained active contours," *IEEE Trans. Medical Imaging*, vol. 23, pp. 1466-1478, 2004.

[4] N. Ray, S. T. Acton, and K. Ley, "Tracking leukocytes in vivo with shape and size constrained active contours," *IEEE Trans. Medical Imaging,* vol. 21, pp. 1222-1235, 2002.

[5] C. Xu and J. L. Prince, "Snakes, shapes, and gradient vector flow," *IEEE Trans. Image Processing,* vol. 7, pp. 359-369, 1998.

[6] C. Xu and J. L. Prince, "Generalized gradient vector flow external forces for active contours," *Signal Processing*, vol. 71, pp. 131-139, 1998.

[7] D. Yuan and S. Lu, "Simulated static electric field (SSEF) snake for deformable models," in *International Conference on Pattern Recognition,* Quebec, Canada, 2002.